

Quantum Melting of Valence Bond Crystal Insulators and Novel Supersolid Phase at Commensurate Density

Arnaud Ralko,¹ Fabien Trouselet,^{2,3} and Didier Poilblanc³

¹ Institut Néel UPR2940, CNRS and Université de Grenoble, F-38000 France

² Max Planck Institut für Festkörperforschung, Heisenbergstrasse 1, D-70569 Stuttgart, Germany

³ Laboratoire de Physique Théorique UMR5152, CNRS and Université de Toulouse, F-31062 France

(Dated: February 22, 2024)

Bosonic and fermionic Hubbard models on the checkerboard lattice are studied numerically for infinite on-site repulsion. At particle density $n=1/4$ and strong nearest-neighbor repulsion, insulating Valence Bond Crystals (VBC) of resonating particle pairs are stabilized. Their melting into superfluid/metallic phases under increasing hopping is investigated at $T = 0K$. More specifically, we identify a novel and unconventional *commensurate* VBC supersolid region, precursor to the melting of the bosonic crystal. Hardcore bosons (spins) are compared to fermions (electrons), as well as positive to negative (frustrating) hoppings.

Understanding the conditions and mechanisms for charge conduction in strongly correlated systems, especially frustrated ones, is a highly non-trivial problem: aside from the strength of interactions, the lattice geometry, but also statistics of charge carriers, can play a relevant role. A case of interest is that of lattices with a pyrochlore-like structure: among those, various unusual electronic phases are encountered, from (insulating) spin liquids [1] to superconductivity, *e.g.* in spinels involving $3d$ electrons as quarter-filled LiTi_2O_4 [2]. Also, other spinels like LiV_2O_4 have heavy-fermion behaviors [3] and are close to a Metal-Insulator (MI) transition [4], raising attention to electronic correlations in a pyrochlore-based geometry.

On the other hand, properties of some half-polarized antiferromagnetic spinels [5] can be described similarly as those of anisotropic (XXZ) magnets on a pyrochlore lattice. In the simplified case of a spin-1/2 XXZ magnet, representing up-(down-)spin by the presence (absence) of a boson, a mapping to hard-core bosons with NN repulsive interactions can be used; an external magnetic field h_z , analog of a bosonic chemical potential, tunes the bosonic density. At $h_z = 0$ and only an Ising coupling on the bonds of the checkerboard lattice of Fig. 1 (the two-dimensional analog of the pyrochlore lattice), the classical ground state (of density $n=1/2$) is highly degenerate and follows the so-called *ice-rule* constraint: the lowest Ising energy corresponds to precisely two bosons on every (flattened) tetrahedron. By tuning h_z to reach a bosonic density of $n=1/4$, again the classical ground-states obey an ice-rule constraint of precisely one particle per tetrahedron (blue tetrahedra of Fig. 1). Second-order processes in the exchange coupling lead to the dynamics of a loop model [6, 7] ($n=1/2$) or of a quantum dimer model (QDM) [8] ($n=1/4$). Note that similar lattice gas picture can also be relevant to easy-axis spin-S systems [9] ($S \geq 3/2$).

A specificity of these local constraints, aside from the finite ground state degeneracy at the classical level, is that charge excitations may *a priori* be fractionalized [10]: adding a particle of charge $-e$ to a system respecting initially the ice-rule creates 2 defects (tetrahedra on which this rule is violated) of fractional charge $-e/2$ which can move to neighboring tetrahedra (Fig. 1). An insulating phase with fractional ex-

citations could thus be considered, close enough to the MI transition such that fractionalization is allowed by kinetic energy gain [11].

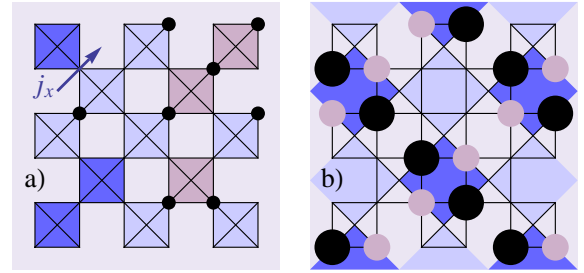


FIG. 1: (Color online). a) Topological defects of fractional charge $+e/2$ (2 particles on a red tetrahedron) and $-e/2$ (empty blue tetrahedron) and particle-hole excitation with two pairs of NN defects. b) Artistic view of the mixed-VBC supersolid phase at commensurate density $n=1/4$ showing inhomogeneous charge density (dots), resonating plaquettes (blue) and superfluid density (light blue).

Lastly, we note that supersolidity has been predicted under doping a charge-ordered bosonic state [12]. *Commensurate* supersolids can be observed as an out-of-equilibrium state of cold atoms [13], or arising from the melting of a conventional charge-ordered insulator [14]. Recent developments of *frustrated* optical lattices of cold atoms [15] open new directions.

To address the above issues, in this Letter we consider Hubbard hamiltonians on the checkerboard lattice in the infinite on-site repulsion (U) limit that reads:

$$H = -t \sum_{\langle i,j \rangle, \sigma} P_G (c_{i,\sigma}^\dagger c_{j,\sigma} + h.c.) P_G + V \sum_{\langle i,j \rangle} n_i n_j, \quad (1)$$

where $c_{i,\sigma}^\dagger$ is a fermion (electron) creation operator at site i , σ its spin index and n_i is the onsite density operator. The Gutzwiller projector P_G enforces the $U=\infty$ limit (no doubly occupied site) [16]. Note that the hopping term t and the nearest neighbor (NN) Coulomb repulsion V have the same magnitude on all bonds. We also consider hardcore bosons (spins) - a bosonic density $n < 1/2$ corresponds to a spin system at

polarization $1 - 2n$) replacing $c_{i,\sigma}$ by bosonic b_i operators and dropping the sum on σ .

Although the lattice is frustrated, the $t > 0$ bosonic model does not suffer from a sign problem and can be addressed using Quantum Monte Carlo (QMC) techniques. In a closely related system, in which bosons hop on the square lattice and interact via bonds on the checkerboard lattice, analytical arguments and finite-T QMC simulations have shown that the system (extrapolated to $T = 0K$) undergoes, at density $n=1/4$, a *weakly first-order* phase transition from a superfluid (SF) phase at small V/t to a large V/t MI phase [17] (which breaks lattice translation symmetry), despite the possibility of being an unusual non-Landau transition [18]. A similar type of phase transition was also found on the Kagome lattice [19]. Here, since the bosons can hop on *all bonds* of the lattice, we performed Green Function QMC (GFQMC) simulations *directly* at $T = 0K$ and *in the canonical ensemble* ($n=1/4$) on clusters up to $14\sqrt{2} \times 14\sqrt{2}$ ($N=392$ sites) to determine the emerging quantum phases. For frustrated $t < 0$ and/or the case of fermions, studies are restricted to smaller clusters, typically $N=32$ sites *for a cluster compatible with all lattice symmetries* which can be handled using Lanczos Exact Diagonalizations (ED) [20].

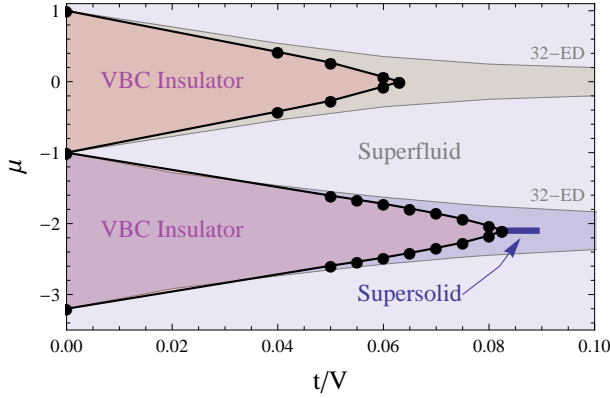


FIG. 2: (Color online). Phase diagram of the $t>0$ bosonic hard-core Hubbard model as a function of the parameter t/V and the chemical potential μ . Extrapolation to the thermodynamic limit (TDL) of $T=0K$ GFQMC results in the canonical ensemble (dots) are compared to ED results. The two lobes correspond to the $n=1/4$ (bottom) and $n=1/2$ (top) VBC insulators (see text). A region of supersolid phase is found at commensurate $n=1/4$ filling (thick segment).

A typical phase diagram of eq.[1] is shown in Fig. 2 where the chemical potential μ has been introduced via a simple Legendre transformation w.r.t. the density. This phase diagram (for $t>0$ bosons, to be discussed later) raises a number of important issues *i.e.* (i) the properties of the insulating VBC in the lobes, (ii) the nature of the phase transition towards the itinerant phases, (iii) the role of the quantum statistics (fermions vs bosons) and (iv) the effect of a frustrating $t<0$ hopping. The paper is organized as follows. First, we investigate the evolution with increasing hopping of the gapped insulating phase towards a compressible fluid. Next, we character-

ize the VBC insulator from various relevant structure factors and discuss the presence of a novel exotic supersolid phase with *coexisting VBC and SF orders*. Third, optics and dipolar excitations are discussed by calculating the optical properties in the VBC insulators and in the itinerant metallic (fermions) or SF (bosons) phases. Finally, we consider the physics of fractional defects beyond the ice-rule constraint. Note that the results shown below refer to $n=1/4$, *i.e.* to a quarter-filled bosonic (1/8-filled fermionic) system.

From the insulator to a compressible fluid – The insulating (incompressible) character of a system manifests itself by a finite gap in the quasiparticle charge excitation spectrum. The gap closes in the metallic (fermions) or SF (bosons) phase [11]. Physically, the process of creating a particle-hole excitation as in Fig. 1(b) by moving a particle from one edge of the sample to the other edge costs a finite energy Δ_C , the charge gap, simply calculated by $\Delta_C = E_+ + E_- - 2E_0$ with the (total) ground state (GS) energies E_0 at filling $n=1/4$, and E_{\pm} with one extra (less) particle. The ED results in Fig. 3(a) show that, both for bosons or fermions, Δ_C decreases linearly with $|t|$ from 2V at $t = 0$ suggesting a transition at finite t to an itinerant GS. Despite the small cluster size some trends can be noticed; (i) the *relative* robustness of the insulator w.r.t. its competing compressible phase does not seem to differ significantly between bosons and fermions and (ii) a frustrating $t < 0$ hopping is much less efficient to destroy the insulator (see also Ref. 20). For unfrustrated bosons, GFQMC calculation can be performed on much larger size clusters (up to 392 sites), at $T = 0K$ and for very small ratio of t/V . A careful size-scaling enables us to extract the TDL of Δ_C , displayed in Fig. 4(a). The transition characterized by the closure of Δ_C is located at $t/V \simeq 0.082$, not so far from its estimation for the square hopping boson model [17]. Note that the width $\Delta\mu$ of the $n=1/4$ and $n=1/2$ insulating lobes of Fig. 2 is given by the extrapolated charge gap.

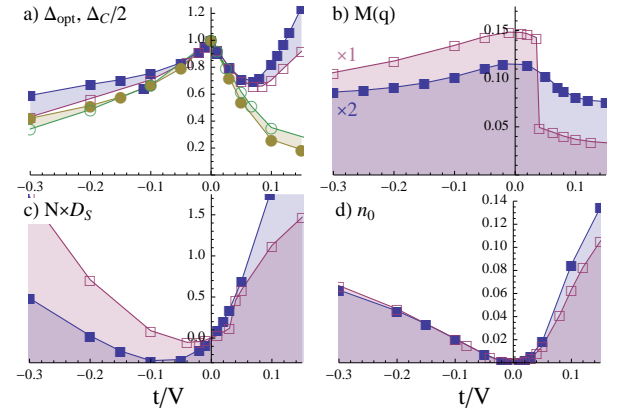


FIG. 3: (Color online). ED results obtained on a 32-site cluster for both fermions (empty symbols) and bosons (filled symbols): a) charge (circles) and optical (squares) gaps, all in units of V , b) order parameter $M_+(K)$, c) Drude weight and d) average number of $-e/2$ charge defects. For fermions, discontinuities due to a level crossing at $t/V \simeq 0.035$ might be a finite size effect.

VBC insulators and supersolid (SS) – As discussed above, at large V/t , mappings to generalized QDM describing the insulating phase are extremely useful to establish the VBC nature of the insulator, in particular its feature of resonating particle pairs at $n=1/4$ [21, 22]. For fermions, spin degrees of freedom play an essential role, since the effective kinetic processes act only on *singlet* electron-pairs on the void plaquettes [20, 22]. The insulators at $n=1/2$ and $n=1/4$ have gapped triplet excitations and the same broken translation symmetries [22] as their bosonic VBC analogs of Refs. 6 and 21. However, when approaching the phase transition by increasing t , the microscopic model (1) becomes necessary since the charge defects of Fig. 1(a) play a crucial role. We then compute the structure factor of the diagonal operator $P_{\pm} = d_i d_j \pm d_k d_l$ defined in a previous work [21], where $d_i d_j$ counts the pair (0 or 1) of particles facing each other across every void plaquette (on the same plaquette at $\pi/2$ angle for $d_k d_l$). Note that in the fermionic case, a projector on the 2-particle $S_z=0$ subspace is implicit in the definition of P_{\pm} . Following the same symmetry considerations as in [21], the s-wave (d-wave) structure factor at point $K=(\pi, \pi)$ ($\Gamma=(0,0)$) signals plaquette ordering (rotational symmetry-breaking). The related order parameters $M_+(K)$ (plaquette) and $M_-(\Gamma)$ (columnar) [23] are defined as

$$M_{\pm}(q) = \sqrt{\frac{1}{N} \langle \psi_0 | P_{\pm}(-q) P_{\pm}(q) | \psi_0 \rangle}. \quad (2)$$

Data of Fig. 3(b) reveal striking differences between $t > 0$ and $t < 0$ with a weaker suppression of the VBC plaquette order parameter with $|t|$ in the frustrated case, following the same trend as Δ_C vs $|t|$. In the bosonic $t > 0$ model, a careful size-scaling analysis of QMC data again enables to extract the TDL of the $T=0K$ order parameters as shown in Fig. 4(b). This evidences clearly that these two order parameters of the mixed columnar-plaquette phase found in the large- V limit [21] melt almost simultaneously at the phase transition around $t/V \simeq 0.089$. Strikingly, the vanishing of the VBC order parameter appears at a larger value than the insulator-SF transition. This shows a persistence of the VBC order within the SF phase, *i.e.* a small region of SS phase. Note that (i) in contrast to the bosonic triangular lattice [12], this phase appears here at a *commensurate* density, (ii) its VBC character strongly differs from usual charge ordering, and (iii) the presence of kinetic processes on the crossed bonds is essential, the VBC insulator-SF transition being weakly first-order otherwise [17] with *no* intermediate phase. However the *exact* equality between the bond strengths within the crossed plaquettes is not crucial and the exotic SS phase should exist in an extended parameter region. We speculate that, for fermions, a similar (narrow) exotic VBC metallic phase might also appear.

Optics – We now analyze the optical conductivity: first, it provides important information on transport, from its $\omega \rightarrow 0$ limit, the Drude weight (its finiteness characterizing a metal or SF). Note that for bosons at $T=0K$, this Drude weight corresponds to the stiffness of superfluidity [24]. Secondly, *neutral dipolar* excitations should appear in the finite frequency

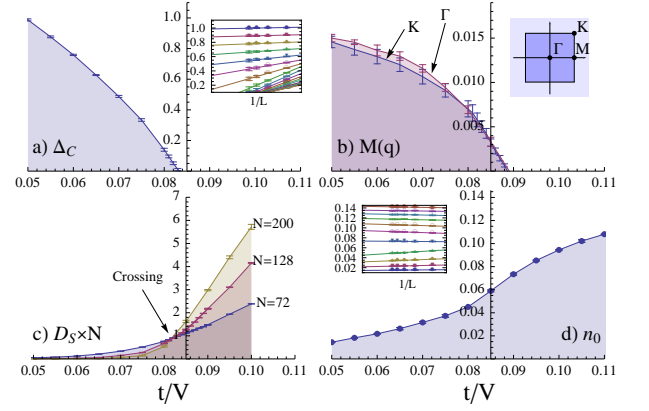


FIG. 4: (Color online). GFQMC results for (hard-core) bosons with $t > 0$. TDL of the charge gap in units of V (a), the order parameters $M_+(K)$ and $M_-(\Gamma)$ with the Brillouin zone depicted in the inset (b), the stiffness parameter rescaled by the number of sites N (c) and the average number of $-e/2$ charge defects (d). The same scale is used to plot these quantities versus t/V to emphasize the transition point close to 0.085. Size-scalings are depicted in the insets.

absorption spectrum. Observe that, for fermions, these excitations are also spin singlets. First, we calculate by Lanczos ED the finite frequency conductivity,

$$\sigma_{x,x}(\omega) = \frac{1}{\omega} \text{Re} \langle \psi_0 | j_x \frac{1}{\omega + i0^+ - H + E_0} j_x | \psi_0 \rangle, \quad (3)$$

where j_x is the current operator along one of the diagonal directions as shown on Fig. 1. The data on Fig. 5 clearly show, at small $|t|/V$, an optical gap $\Delta_{\text{opt}} \sim V$ corresponding to an absorption energy threshold. As shown in Fig. 3(a), this gap follows closely - for small enough $|t|/V$ - the linear behavior with $|t|$ of Δ_C . We believe the up-turn at $t/V \sim 0.08$ indicates the transition to the metallic/superconducting phase, where the energy scale of excitations cross-over from V to t .

Interestingly, low-energy peaks are observed in $\sigma(\omega)$ below Δ_{opt} at energies $\sim t^2/V$ set by the effective QDM hamiltonian. While such $q=(0,0)$ low-energy dipolar excitations correspond to usual excitations of a metal/SF, it is not clear yet whether they would also survive in the TDL in the insulator, as occurring from local charge fluctuations.

The Drude weight D_S , extracted from the above ED results via the optical sum rule and plotted in Fig. 3(c), increases rapidly with $|t|/V$ but does not allow to locate the insulator-metal (or SF) transition for such small systems. Fortunately, in the case of bosons and $t > 0$, it is possible to compute the Drude weight with the GFQMC method using the winding numbers of the flow of the particles in imaginary time τ [24]. At a continuous solid to SF transition, the stiffness scales as $D_S = L^{-z} f(L^{1/\nu} (t/V - (t/V)_c), \tau L^z)$ with the dynamical z and the correlation length ν exponents [19]. Searching for a universal behavior of f w.r.t. L , we obtain a very accurate estimation of the transition at $t/V \simeq 0.082$ (crossing in Fig. 4(c)), with $z = 2$ and $\nu = 1/2$. In agreement with the vanishing of Δ_C , this is an extra evidence in favor of a win-

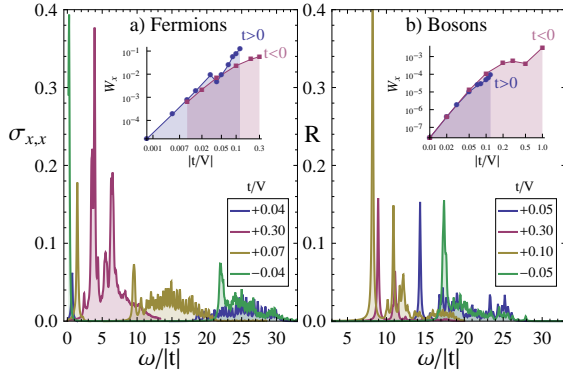


FIG. 5: (Color online). $\sigma(\omega)$ for a) the fermions and b) the bosons at different values of t/V (ED on a 32-site cluster). Insets: relative weight of the low-energy dipolar matrix elements (only visible for fermions on the $\sigma(\omega)$ plot), plotted vs t/V in log-log scale.

dow of width $\Delta(t/V) \simeq 7 \cdot 10^{-3}$ of a SS phase exhibiting a finite SF stiffness D_S and $\Delta_C = 0$ but with two finite VBC order parameters.

The physics of fractional defects – Within the effective QDM, the amplitude of dimer flips (*i.e.* simultaneous 2-particle move on a void plaquette [6]) goes like t^2/V . Hence, the concentration n_0 of $\pm e/2$ defects (*cf* Fig. 1(a)) shows in Fig. 3, for very small t , a $(t/V)^2$ behavior, symmetrically for $t > 0$ and $t < 0$. However, as soon as $|t|/V > 0.03$, the observed behaviors are beyond the physics of the effective QDM. Nevertheless, the phase transition occurs at a small t/V value so that the ice-rule constraint should still operate in the metallic/SF phase which contains only ~ 6 -10% of fractional defects. Since the deconfinement [17] of these defects occurs at the vanishing of the VBC order parameter, they should still be confined in the SS phase.

We summarize here the main findings of this work. First, a strong asymmetry is found between $t > 0$ and $t < 0$, a frustrated hopping ($t < 0$) being less efficient to melt the VBC insulator. This originates from a relatively smaller increase with $|t|$ of the average kinetic energy and concentration n_0 of fractional charged defects, as shown in Fig. 3(d). Secondly, for the non frustrated $t > 0$ bosonic model, evidence are provided for a *double* quantum phase transition between the VBC insulator at small t and the SF at large t , involving an intermediate *commensurate* [25] supersolid phase breaking *both* translation and rotational symmetries. Its VBC character (anisotropic resonating plaquettes) clearly distinguishes it from its charge ordered counterpart [14]. We speculate that such a feature should be present in the frustrated $t < 0$ case and/or for fermions (with an intermediate VBC metal). Lastly, optical properties are investigated, showing an optical gap following the behavior of the charge gap.

Acknowledgements – We thank K. Damle, P. Fulde, N.

Laflorencie and S. Wessel for interesting discussions. F.T. is grateful to IDRIS (Orsay, France) for computer time.

-
- [1] P. Mendels *et al.*, Phys. Rev. Lett. **98**, 077204 (2007).
 - [2] D. C. Johnston, J. of Low Temp. Phys. **25**, 145 (1976).
 - [3] P. Fulde *et al.*, Eur. Phys. Lett. **54**, 779 (2001).
 - [4] P.E. Jönsson *et al.*, Phys. Rev. Lett. **99**, 167402 (2007).
 - [5] H. Ueda *et al.*, Phys. Rev. Lett. **94**, 047202 (2005); D. L. Bergman *et al.*, Phys. Rev. Lett. **96**, 097207 (2006).
 - [6] N. Shannon, G. Misguich, K. Penc, Phys. Rev. B **69**, 220403(R) (2004); O. F. Syljuasen, S. Chakravarty, Phys. Rev. Lett. **96**, 147004 (2006).
 - [7] The SU(2) antiferromagnet corresponds to $t/V = -0.5$ and $c_{i\sigma} \rightarrow b_i$ in Eq. (1). On the checkerboard lattice and for zero field (*i.e.* $n=1/2$), its GS is a singlet VBC with alternating resonating void plaquettes (see J.-B. Fouet *et al.*, Phys. Rev. B **67**, 054411 (2003)) continuously connected to the $|t| \ll V$ Ising analog of Ref. 6.
 - [8] D.S. Rokhsar and S.A. Kivelson, Phys. Rev. Lett. **61**, 2376 (1988).
 - [9] A. Sen, K. Damle, A. Vishwanath, Phys. Rev. Lett. **100**, 097202 (2008).
 - [10] P. Fulde, K. Penc, N. Shannon, Ann. Phys. **11**, 892 (2002); F. Pollmann, P. Fulde, E. Runge, Phys. Rev. B **73**, 125121 (2006).
 - [11] Ice-rule constraints bring novel features w.r.t. the bandwidth-controlled Mott transition at half-filling ($n=1$) described *e.g.* in T. Yoshioka, A. Koga, N. Kawakami, J. Phys. Soc. Jpn. **77**, 104702 (2008).
 - [12] S. Wessel and M. Troyer, Phys. Rev. Lett. **95**, 127205 (2005); D. Heidarian and K. Damle, Phys. Rev. Lett. **95**, 127206 (2005).
 - [13] T. Keilmann, I. Cirac, T. Roscilde, Phys. Rev. Lett. **102**, 255304 (2009).
 - [14] K.-K. Ng and Y.C. Chen, Phys. Rev. B **77**, 052506 (2008).
 - [15] J. Ruostekoski, Phys. Rev. Lett. **103**, 080406 (2009).
 - [16] At *finite* U , small V and large-enough antiferromagnetic coupling $\sim 4t^2/U$, physics is governed by magnetic frustration instead of ice-rule. See M. Indergand *et al.*, Phys. Rev. B **75**, 045105 (2007) for fermions at $n=1/2$.
 - [17] A. Sen, K. Damle, T. Senthil, Phys. Rev. B **76**, 235107 (2007); S. Wessel, Phys. Rev. B **78**, 075112 (2008).
 - [18] T. Senthil *et al.*, Science **303**, 1490 (2004); *ibidem* Phys. Rev. B **70**, 144407 (2004).
 - [19] S. V. Isakov *et al.*, Phys. Rev. Lett. **97**, 147202 (2006).
 - [20] D. Poilblanc, Phys. Rev. B **76**, 115104 (2007).
 - [21] A. Ralko, D. Poilblanc, R. Moessner, Phys. Rev. Lett. **100**, 037201 (2008), A. Ralko, M. Mambrini and D. Poilblanc, Phys. Rev. B **80**, 184427 (2009).
 - [22] D. Poilblanc, K. Penc, N. Shannon, Phys. Rev. B **75**, 220503(R) (2007); F. Trouselet, D. Poilblanc, R. Moessner Phys. Rev. B **78**, 1195101 (2008).
 - [23] Plaquette and columnar orders show *both* in the charge structure factor at momentum $(\pi, 0)$; see *e.g.* Refs. 17, 20.
 - [24] M. Capello *et al.*, Phys. Rev. Lett. **99**, 056402 (2007).
 - [25] The theorem ruling out commensurate supersolids only applies to *continuous* translation symmetry breaking. See N. Prokof'ev and B. Svistunov, Phys. Rev. Lett. **94**, 155302 (2005).